



A tableability change classification system in supporting the tablet formulation design via the roll compaction and dry granulation process

Junhui Su^{a,b}, Kunfeng Zhang^a, Feiyu Qi^a, Junjie Cao^a, Yuhua Miao^c, Zhiqiang Zhang^d, Yanjiang Qiao^{a,b,*}, Bing Xu^{a,b,*}

^a Department of Chinese Medicine Informatics, Beijing University of Chinese Medicine, Beijing 100029, PR China

^b Beijing Key Laboratory of Chinese Medicine Manufacturing Process Control and Quality Evaluation, Beijing 100029, PR China

^c The International Department, No. 8 Middle School of Beijing, Beijing 100045, PR China

^d Beijing Tcmages Pharmaceutical Co. LTD, Beijing 101301, PR China

ARTICLE INFO

Keywords:

Tableability change classification system (TCCS)
Material library
Roll compaction and dry granulation (RCDG)
Formulation design
Risk decision tree

ABSTRACT

In this paper, the material library approach was used to uncover the pattern of tableability change and related risk for tablet formulation design under the roll compaction and dry granulation (RCDG) process. 31 materials were fully characterized using 18 physical parameters and 9 compression behavior classification system (CBCS) parameters. Then, each material was dry granulated and sieved into small granules (125–250 μm) and large granules (630–850 μm), respectively. The compression behavior of granules was characterized by the CBCS descriptors, and were compared with that of ungranulated powders. The relative change of tableability (CoT_r) index was used to establish the tableability change classification system (TCCS), and all materials were classified into three types, i.e. loss of tableability (LoT, Type I), unchanged tableability (Type II) and increase of tableability (Type III). Results showed that approximately 65% of materials presented LoT, and as the granules size increased, 84% of the materials exhibited LoT. A risk decision tree was innovatively proposed by joint application of the CBCS tableability categories and the TCCS tableability change types. It was found that the LoT posed little risk to the tensile strength of the final tablet, when Category 1 or 2A materials, or Category 2B materials with Type II or Type III change of tableability were used. Formulation risk happened to Category 2C or 3 materials, or Category 2B materials with Type I change of tableability, particularly when high proportions of these materials were involved in tablet formulation. In addition, the risk assessment results were verified in the material property design space developed from a latent variable model in prediction of tablet tensile strength. Overall, results suggested that a combinational use of CBCS and TCCS could aid the decision making in selecting materials for tablet formulation design via RCDG.

1. Introduction

Granulation is important in manufacturing of pharmaceutical oral solid dosage (OSD) forms and possesses the advantages of improving pharmaceutical materials' bulk density and flow properties as well as preventing segregation of active pharmaceutical ingredients (APIs) and dust formation (Parikh, 2021). Among various granulation techniques, roll compaction and dry granulation (RCDG) is widely used in the pharmaceutical industry and consists of a compaction step and a milling step. The main advantages of RCDG are the absence of water or other solvents and cost-intensive drying steps, making this technique feasible

for moisture- and/or heat-sensitive materials (Kleinebudde, 2004). Moreover, RCDG is an inherently continuous process which is benefit to pharmaceutical continuous manufacturing (Vervae and Remon, 2005). Besides a large amount of fines, the main drawback of RCDG is the decrease in tensile strength (TS) of tablets produced from dry granules compared to tablets compressed directly from the equivalent powder mixture, which is generally termed as loss of tableability (LoT) or loss of reworkability (Herting and Kleinebudde, 2008; Malkowska and Khan, 1983; Sun and Kleinebudde, 2016).

Various hypotheses had been proposed to interpret the mechanism of LoT, including the work hardening (Malkowska and Khan, 1983), the

* Corresponding author at: School of Chinese Materia Medica, Beijing University of Chinese Medicine, No.11, North Third Ring East Road, Beijing City 100029, PR China.

E-mail address: xubing@bucm.edu.cn (B. Xu).

<https://doi.org/10.1016/j.ijpx.2023.100204>

Received 24 May 2023; Received in revised form 26 July 2023; Accepted 27 July 2023

Available online 28 July 2023

2590-1567/© 2023 The Authors. Published by Elsevier B.V. This is an open access article under the CC BY license (<http://creativecommons.org/licenses/by/4.0/>).

granules hardening (Patel et al., 2011) and the particle size enlargement (Sun and Himmelspach, 2006). Malkowska and Khan (1983) first explained the tableability reduction phenomenon with the work hardening theory and described work hardening as the increased resistance to recompression, because of the entanglement of dislocations on the particle level. However, there were difficulties in demonstrating the presence of lattice dislocations in dry granulation. Instead, Patel et al. proposed the hypothesis of granule hardening, which was mainly related with the reduction of granule porosity (Patel et al., 2011). Sun et al. ascribed the LoT phenomenon of plastic materials to granule size enlargement which led to the reduction in surface area available for bonding in tablet (Sun, 2008; Sun and Himmelspach, 2006). Herting and Kleinebudde (2008) proposed that the LoT was a combination of granules hardening and particle size enlargement. On the basis of previous research, Sun stated that the tensile strength of the tablet was determined by the interaction of the bonding area and bonding strength (BABS) within the tablet, and proposed the use of the BABS principle to understand of the LoT in dry granulation (Sun, 2011). By preparing microcrystalline cellulose (MCC) particles with different porosity structures and studying the loss of their tableability, Nordstrom and Alderborn (2015) found that the particles with more than a certain porosity almost completely collapsed into primary particles in the subsequent compression process, thus leaving the material tableability unchanged, and thus proposed the concept of critical porosity. This was further extended by Tofiq et al. that the microstructure of granules resulted from the primary-to-secondary size enlargement process dictated the tableting performance of dry granulated materials (Tofiq et al., 2022a, 2022b).

Generally, no single mechanism could explain all observations. Different material properties and process parameters might lead to different deformation behaviors of materials after dry granulation, affecting the dominant mechanism of the LoT after RCDG. In practice, understanding the re-compression properties of different materials is beneficial to designing a balanced and robust formulation. Janssen et al. compared the re-compactibility of 8 materials including 3 types of anhydrous lactose, 3 types of lactose monohydrate and 2 types of MCC, and found that tablet tensile strength of lactose only decreased with 7–29%, while tablet tensile strengths of MCC were decreased by 90% at relatively high specific compaction force of 16 kN/cm (Janssen et al., 2022). Palugan et al. evaluated the compaction ability of 4 grades of mannitol, and it was found that the powder and granular mannitol showed lesser compaction ability than the spray dried mannitol, but the spray dried mannitol were more sensitive in losing tableability after dry granulation (Palugan et al., 2022). Grote and Kleinebudde studied the influence of 4 kinds of alpha-lactose monohydrate on tablet properties after RCDG (Grote and Kleinebudde, 2019). The results showed that RCDG of lactose monohydrate with D_{50} of 131 μm and milled lactose monohydrate with D_{50} of 33 μm increased and decreased the tableability, respectively. Omar et al. revealed that the amorphous part in the lactose powder would crystallize at high relative humidity (RH) value (i. e. 80%), which resulted in the loss of powder compressibility (Omar et al., 2016). The authors suggested that the optimum RH conditions for lactose were in the range of 20–40%. Some excipients with high porosity or small primary particles, such as anhydrous lactose with aggregates of microcrystals (Janssen et al., 2022), agglomerated lactose monohydrate (Grote and Kleinebudde, 2019) and functional calcium phosphate dibasic (DCP) agglomerate (Grote and Kleinebudde, 2018), were sensitive to specific compaction force applied and were suitable for RCDG and further tableting in most cases. Heiman et al. (Heiman et al., 2015) investigated the suitability of roller compaction for high drug loading formulations containing two active pharmaceutical ingredients, and it was shown that the loss in compactibility for the brittle API paracetamol was more pronounced than the plastic API ibuprofen. The possible reasons might be that the granulation of ibuprofen did not generate large particles and the resulted ibuprofen granules were more porous compared to the paracetamol granules.

Recently, the material library or material database approach has been brought forward to speed up the development of formulations and processes for new drug products. This approach mainly involves three steps. The first step is to build a material property database including maximal variability of the underlying raw material dataset. For instance, Basu et al. firstly developed a publicly accessible excipients database named the NIPTE-FDA excipients knowledge base, which provided the formulation scientists with comprehensive properties of >70 commonly used excipients (Basu et al., 2011). Suñé Negre established a material database consisting of 51 directly compressible excipients, and each material was characterized by 12 parameters from the SeDeM expert system (Suñé Negre et al., 2014). Van Snick et al. characterized 55 pharmaceutical powders including 18 APIs and 38 excipients that were commonly used in direct compression (DC) and wet granulation (WG) processes, and each material was described by over 100 material descriptors (Van Snick et al., 2018). In the next step, quantitative correlation models could be constructed by linking physical properties of raw materials to unit operations and final product performance. The materials used in such models could be all materials in the material library, or could be a representative material subset selected by the material sparing approaches (Dhondt et al., 2022b; Wang et al., 2019). Currently, the process models on the basis of the material library approach were mainly implemented on single unit operations, such as the direct compression process (Dhondt et al., 2022a; Hayashi et al., 2021; Paul et al., 2019), the roller compaction process (Yu et al., 2019), etc. At last, the obtained process knowledge or process models can enable in-silico exploring the material properties space and the process parameters space (Dai et al., 2019a), help predict process and product performance, reduce the impact of raw material variability on the drug product quality (Zhang et al., 2019) or avoid potential process failures (Hancock, 2019). As far as we know, the material library approach has not been used in the dry granulation processing route toward tablet preparation.

This paper is a continuation of our previous work (Wang et al., 2022) which focused on the change of tableability in the wet granulation process. Considering the fact that some materials (e.g. levetiracetam (Kuntz et al., 2011) or C*PharmMannidex 16,700 (Souhihi et al., 2013)) exhibited increased tableability after roll compaction and dry granulation, the phenomenon of increase or loss of tableability of material after dry granulation were generalized as change of tableability. The purpose of this article was to use the material library approach to understand the patterns of tableability change for different materials processed by roll compaction and dry granulation, clarify the potential risk for tablet formulation design via the RCDG manufacturing route. The rest of this paper was organized as follows: Section 2 introduces the details of the material library, the experimental conditions of RCDG and tableting processes, as well as the methods for characterizing tablet quality, compaction behavior and change of tableability. In Section 3, the physical properties and compaction behavior of 31 materials were studied in detail. Then, the CBCS parameters of granules and ungranulated powders were compared by multivariate analysis. Afterwards, the change of tableability for different materials were classified. Finally, a risk decision tree and a predictive model were constructed to assess the risk of tablet failure of the materials and aid decision making in RCDG tablet formulation design. Section 4 sums up the paper and gives future research directions.

2. Materials and methods

2.1. Materials

31 pharmaceutical materials, including 16 pharmaceutical excipients and 15 natural product powders (NPPs), were chosen to build a material library. In order to create a material library with representative samples, commonly used excipients with different functions such as diluents, binders and disintegrants were selected, like MCC, lactose, hydroxypropyl methylcellulose (HPMC), low-substituted hydroxypropyl

cellulose (L-HPC), croscarmellose sodium (CCNa), corn starch, D-sorbitol, DCP and sodium bicarbonate (NaHCO₃). 4 types of MCC and 5 types of lactose were included in the material library to expand the variation coverage of physical properties. 15 batches of NPPs prepared from 12 medicinal plant materials were provided by the Beijing Tcmages Pharmaceutical Co., Ltd. (Beijing, China). All NPPs were manufactured by pretreatment of medicinal herbs, water extraction, filtration, concentration and spray drying and could be used as raw materials for the fabrication of oral solid dosage of Chinese medicine products (Xiong et al., 2022; Yu et al., 2021; Zhang et al., 2022; Zhao et al., 2023). Compared to excipients, NPPs often possessed high hygroscopicity and poor flowability (Li et al., 2018) and could expand the physical property space of the material library. The name, lot number and supplier for each material are provided in Table S1 in Supplementary Materials.

2.2. Characterization of powders

Each material used in the material library was subject to a series of characterization techniques to determine their physical properties. Among them, 12 parameters were measured or calculated according to the SeDeM expert system methodology^[39], and they were density parameters (bulk density, D_b ; tapped density, D_t), compressibility parameters (inter-particle porosity, I_e ; cohesion index, I_{cd} ; Carr index, IC), flowability parameters (Hausner ratio, IH ; angle of repose, AoR ; flow time, F'), stability parameters (moisture content, %HR; hygroscopicity, %H) and uniformity parameters (particle size <50 μm , %Pf; homogeneity index, $I\theta$). In addition, other 6 parameters, i.e. the true density (ρ_t), solid fraction for powder (SF_p), particle sizes D_{10} , D_{50} , D_{90} and $Span$ were also used to describe the properties of powders. The testing procedures of above 18 parameters were thoroughly described by Dai et al. (2019b). The characterization data of all materials are from the iTCM database and are shown in Table S2 in Supplementary Materials.

2.3. Roll compaction and dry granulation

Roll-compacted ribbons were manufactured using a LGS120 roll compactor (Beijing Longli Tech Co., Ltd., Beijing, China), equipped with a hopper, a horizontal feed screw, two knurled rim rolls (120 mm in diameter and 35 mm in width), and rim roll sealing. During ribbon production, the roll compactor was set to the roll speed of 6 rpm, the feed screw speed of 20 rpm, and the hydraulic pressure of 70 bar, while the roll gap varied according to the feed material properties. In order to avoid sticking, the roll surface was lubricated by magnesium stearate and the temperature of the rolls was controlled by using a circulating water-cooling system. Samples were collected when the material had completely submerged the feed screw and the ribbon production had been stabilized.

The produced ribbons were manually broken into smaller pieces and then fed into a conical mill granulator with a 2.0 mm sieve screen and the impeller speed set at 300 rpm. Granules were collected and were further sieved into fractions of 125–250 μm and 630–850 μm (Grote and Kleinebudde, 2018; Herting and Kleinebudde, 2008; Sun and Himmelspach, 2006) using an automatic shaking screen (ZNS-300, Beijing Xinghelishi Tech & Dev Co., Ltd., Beijing, China). The sieving time was 5 min, and the vibration frequency was 30 Hz. The collected granules were put into a ziplock bag and were stored at room temperature with relative humidity lower than 40% for subsequent investigations.

2.4. Compression of tablets

The powdered materials or dry granulated granules were compressed into tablets using a single punch tablet press (C&C600A, Beijing C&C CAMBCAVI Co., Ltd., China) equipped with 10 mm flat faced punches. The applied mean velocity of the upper punch was 28 mm·s⁻¹. Tablets of each material were compressed at the weight of 350 \pm 5 mg and were manually filled into the die, while powders with bulk densities below

0.35 g·mL⁻¹ were compressed with fill weight of 300 \pm 5 mg. The compression force was controlled by adjusting the distance between the upper and lower punches and the accurate pressure was measured through a compression force transducer and was displayed on the control panel. Five compression forces in the range of 3 \times 10²–11 \times 10³ N (approximately 40–140 MPa) were used to produce tablets with different hardness. The punch surfaces and die walls were lubricated externally with magnesium stearate before each compression. After ejection, tablets were placed in an airtight container for at least 48 h to allow for elastic recovery prior to measurement of dimensions and crushing force.

2.5. Characterization of tablets

The tablet thickness (H , in mm) and diameter (D , in mm) were measured by a digital thickness gauge (547–401 Digimatic Caliper, Mitutoyo, Japan) and the tablet weight (m , in g) was measured using an electronic balance (GL124-1SCN, Beijing Sanfu Hezhong Technology Development Co., China). The diametrical breaking force (F , in N) of a tablet was measured using the tablet hardness tester (YPD-500, Shanghai Huanghai Medicine Inspection Instrument Co., Ltd., China) and the tensile strength (TS) of tablet was calculated according to eq. 1 (Fell and Newton, 1970).

$$TS = \frac{2F}{\pi DH} \quad (1)$$

where F , D , H , as defined above, were the diametrical breaking force, the tablet diameter and the tablet thickness, respectively.

The solid fraction (SF) was calculated based on the tablet weight, dimensions, and the true density of the powder (ρ_p) using eq. 2. SF was also called the relative density of the tablets. The tablet porosity (ϵ) could be obtained according to eq. 3.

$$SF = \frac{\rho_{app}}{\rho_t} = \frac{4m}{\pi D^2 H \rho_t} \quad (2)$$

$$\epsilon = 1 - SF \quad (3)$$

where ρ_{app} indicated the apparent density of the tablet. ρ_t was defined as the true density of tablet, which was equal to the true density of the starting material.

2.6. Compaction behavior evaluation

Each material was compressed under the conditions described in Section 2.4 and tablet characterizations were carried out according to Section 2.5. The tensile strength and porosity of the tablets under various compression pressures could be obtained. The compression behavior classification system (CBCS) technique was used to evaluate the compression properties of the material (Dai et al., 2019a). In CBCS, the compression and compaction behavior of materials was characterized from three aspects: the compressibility (porosity-compression pressure relationship), the compactibility (porosity-tensile strength relationship) and the tabletability (tensile strength-compression pressure relationship). By fitting equations listed in Table 1, nine CBCS descriptors are calculated for every material. The curve fitting performance was evaluated by the coefficient of determination (R^2).

2.7. Characterization of tabletability change

Currently, there have been four methods for characterizing the change of tabletability: (1) The reworking potential (Malkowska and Khan, 1983), (2) The ratio of slope of the tabletability curve of granules to that of powders (Hein et al., 2008), (3) The ratio of tensile strength of tablets made of granules to that of powders under the same compression pressure (Herting and Kleinebudde, 2007), and (4) the relative change of

Table 1
The compression equations used to calculate the CBCS parameters.

Compaction behavior	Equation	Compression parameter
Compressibility	Heckel $\ln \frac{1}{\epsilon} = KP + A$	$P_y, \frac{P_y}{K}$
	Gurnham $\epsilon = \frac{1}{K} \ln \left(\frac{P}{P_0} \right)$	K
	Kawakita $\frac{P}{C} = \frac{1}{ab} + \frac{P}{a}$	a, ab, b^{-1}
Compactibility	Shapiro $\ln(\epsilon) = \ln \epsilon_0 - kP - fP^{0.5}$	f
	Ryskewitch-Duckworth $TS = T_0 \exp(-k_b \epsilon)$	k_b
Tabletability	Power $TS = dP^g$	d, g

tabletability (Wang et al., 2022).

Fig. 1 depicts the calculation method for the reworking potential (RP) and the relative change of tabletability (CoT_r). The padding part A is the area under the tensile strength vs. pressure curve of powdered materials, and it is denoted by AUC_p . The padding part B is the area under the tensile strength vs. pressure curve of granules, which is denoted by AUC_g . For a given material, the padding part (B-A) represents its change of tabletability which can be calculated by ($AUC_g - AUC_p$).

The area under the lowest tensile strength vs. pressure curve in the material library is defined as AUC_{min} , and the area under the highest tensile strength vs. pressure curve is defined as AUC_{max} . The padding part C represents the area between the highest and the lowest tensile strength vs. pressure curves in the material library.

The reworking potential is calculated using eq. 4, which denotes the ratio of area under the tabletability curve of granules to that of powders.

$$RP = \frac{B}{A} = \frac{AUC_g}{AUC_p} \times 100\% \quad (4)$$

CoT_r is calculated by eq. 5, which denotes the ratio of the area between AUC_g and AUC_p to the area between AUC_{max} and AUC_{min} .

$$CoT_r = \frac{B - A}{C} = \frac{AUC_g - AUC_p}{AUC_{max} - AUC_{min}} \times 100\% \quad (5)$$

2.8. Multivariate analysis

In this study, the principal component analysis (PCA) was used to reveal latent structures in the data set and identify potential groups of materials. The partial least squares (PLS) regression method was used to

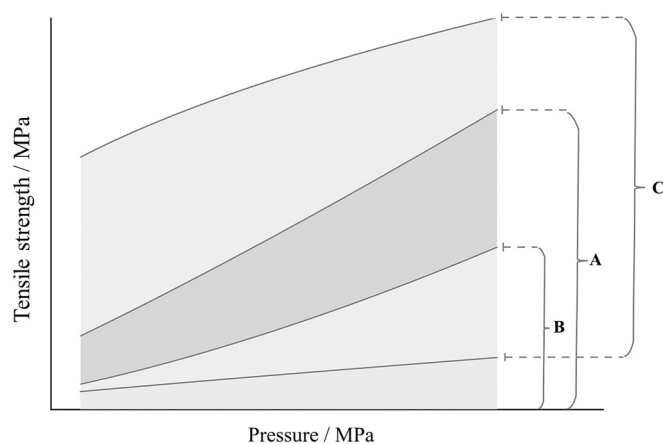


Fig. 1. Schematic diagram of the calculation method of reworking potential and relative change of tabletability.

develop the relationship between the matrix of independent variables and the matrix of dependent variables. Multivariate data analysis was performed on the SIMCA 14.1 software (Umetrics, MKS, Umea, Sweden).

3. Results and discussions

3.1. Powder physical properties

As illustrated in Section 2.2, each powdered material was characterized by 18 physical parameters. Six representative parameters were selected as examples to express the diversity of the material library. The histograms of the six parameters are shown in Fig. 2.

The particle size and the *Span* were important factors that affected the compaction behavior of the material (Dai et al., 2019a). It can be seen in Fig. 2(A) that D-sorbitol (No. E15) lying on the far right of the X-axis has the largest median particle size (D_{50}) of 376.7 μm . The median particle sizes of remaining 30 materials were spread in the range between 8.68 μm (Scutellariae Radix, No. Z15) and 177.2 μm (MCC PH102 SCG, No. E1). Besides, 21 materials in the material library had the median particle sizes $<50 \mu\text{m}$. Distinct from excipients, which had broad D_{50} distribution from 12.6 μm to 367.7 μm , the D_{50} values of all NPPs were concentrated in a smaller range between 8.68 μm and 39.6 μm .

As shown in Fig. 2(B), the hygroscopicity values are ranged from near zero (Lactose Flowlac 100 that was abbreviated as Lac F100, No. E5) to 18.97% (Sophorae Flavescentis Radix, No. Z12). Four batches of lactose possessed the hygroscopicity values lower than 1.0%, indicating the excellent stability of lactose materials. The 15 batches of NPPs had relatively high hygroscopicity values that were larger than 9.50%. The high moisture sensitivity of NPPs might be related to the hydrophilic components in the water extracts (Atanasov et al., 2021), as well as their smaller particle sizes and larger specific surface areas.

The bulk density is used to indicate voids within and between particles, and the packing ability of bulk materials. The packing properties of powders varied from the very loosely packed Scutellariae Radix powder (No. Z15, 0.22 $\text{g}\cdot\text{mL}^{-1}$) to the densely packed DCP powder (No. E16, 0.91 $\text{g}\cdot\text{mL}^{-1}$). Powders that had higher structural strength and greater inter-particle friction could withstand collapsing, resulting in a lower bulk density. Generally, high bulk density was conducive to improving the powder's manufacturability. For instance, the manufacturing classification system (MCS) summarized that materials with a bulk density $>0.50 \text{ mL}^{-1}$ were suitable for the direct compression process (Leane et al., 2015).

The true densities of 31 materials were spread in the range between 1.17 $\text{g}\cdot\text{cm}^{-3}$ (Atractylodis Rhizoma, No. Z8) and 2.91 $\text{g}\cdot\text{cm}^{-3}$ (DCP, No. E16). Except for DCP, NaHCO_3 (No. E14) had relatively large true densities that was 2.23 $\text{g}\cdot\text{cm}^{-3}$. The solid fraction (SF_p) was a measure of solid content of materials and was typically higher for materials with a higher bulk density, but a lower true density. The material with the smallest solid fraction was Scutellariae Radix (No. Z15, 0.15), and the largest was Angelicae Sinensis Radix (No. Z3, 0.47). Powders with larger solid fractions, such as Lac F100 (No. E5, 0.40) and Lactose Anhydrous 21 AN (Lac 21 AN, No. E6, 0.45), were denser and might weaken the plastic deformation ability during compression.

The *Icd* values for all materials varied between 14.3 N (corn starch, No. E11) and 366.8 N (MCC PH102 SCG, No. E1). Within the research scope, six batches of cellulose materials had high *Icd* values that were all $>162.9 \text{ N}$. A large *Icd* value suggested a material had adequate compressibility. Yet, the *Icd* values of four kinds of powders were $<50 \text{ N}$, and these powders were corn starch (No. E11), Lactose Granulac 200 (Lac G200, No. E7), NaHCO_3 (No. E14), and DCP (No. E16). Their small *Icd* values might be related to the powder's inability to bond adequately under certain compression conditions (Nofrierias et al., 2018). DCP was demonstrated to be weakly compressible because it was extremely hard to densify below a porosity of 0.3 (Reynolds et al., 2017).

Furthermore, physical properties of 31 materials were combined into

powders with low density values were easy to be compressed. The flowability and hygroscopicity parameters contributed to PC3 to a large extent. The hygroscopicity parameter was located at a near 90-degree angle with Icd , indicating that they were almost uncorrelated. The score plot for the first three PCs is shown in Fig. 3(B). The NPPs in green dots are positioned in the bottom-left part of the latent variable space, while the excipients in yellow dots are widely scattered. The NPPs exhibited clearly different physical properties compared to the commonly used excipients. In consideration of the corresponding relationship between the score plot and the loading plot, the NPPs were observed to preserve small particle sizes, high hygroscopicity and low densities. Overall, the results proved that the material library provided a material physical properties space full of information and diversity.

3.2. Compaction behavior of powders

In order to thoroughly characterize the compaction behavior of each powder, different compression equations listed in Table 1 are fitted to derive the CBCS parameters, and the goodness of fit values are provided in Table S3 of the Supplementary Materials.

The relationship between tablet porosity and compression pressure serves as a representation of the compressibility of a powder, which is the capacity to apply pressure to reduce its volume (Joiris et al., 1998). The Kawakita ab parameter, also known as the rearrangement index, could be used to indicate the incidence of particle rearrangement at low compression pressures during the initial compression and a high value of ab corresponds to a high potential for particle rearrangement (Nordstrom et al., 2009). The ab parameters for 31 powdered materials in the material library ranged from 0.06 (Polygoni Multiflori Radix Praeparata, No. Z9) to 0.35 (HPMC). The corn starch had a low ab value (i.e. 0.09), which was similar to the ab index for the maize starch (i.e. 0.08) reported by Klevan et al. (2010), meaning that the starch material had limited initial particle rearrangement. Besides, most of the NPPs (No. Z1-Z3, Z5-Z14) had ab values lower than 0.10, which was inconsistent with findings that a powdered material below the critical threshold of particle size (i.e. 40 μm) was prone to rearrangement (Nordstrom et al., 2009). This phenomenon could be explained by the fact that the rearrangement of NPPs may happen at even lower pressures during the manual filling stage before compression.

The degree of particle fragmentation at low compression pressure (0–50 MPa) was indicated by the index of Shapiro f . The values of Shapiro f varied substantially from 0.0873 (CCNa) to 0.4202 (Lactose Pharmatose 200 M that was abbreviated as Lac P200M, No. E9). Lac P200M is milled lactose monohydrate with a D_{50} value of 46.6 μm , and it has a significant tendency to fragment during compression. The resistance to densification under applied pressure was described by the plasticity parameter P_y , which was calculated from the Heckel equation. The P_y values for the material library ranged from 74.1 MPa (MCC PH102) to 476 MPa (DCP). Two batches of NPPs (No. Z5, 74.5 MPa; No. Z10, 75.5 MPa) and two batches of excipients (i.e. MCC PH102 and MCC PH302) were classified into soft materials. Most NPPs fell within the category of the moderately hard. The mean P_y value of NPPs (i.e. 123 MPa) was lower than that of excipients (195 MPa), and the mean f value of NPPs (i.e. 0.184) was also lower than that of excipients (i.e. 0.266), indicating that the texture of NPPs was relatively soft and NPPs were not easy to fragment.

The relationship between tablet tensile strength and tablet porosity during the compaction process was described by the R-D equation. The derived k_b parameter was used to reflect the bonding capacity between particles. A higher k_b value implies that the powders possess inferior bonding capacity. The MCC PH102 had the lowest k_b value (4.89), and the NaHCO_3 had the highest k_b value (15.6). Generally, the cellulose materials such as MCC, HPMC and L-HPC had favorite compactability properties, since their k_b values were <9.05 . By contrast, the lactose materials and inorganic salts had relatively weak bonding capacities. The k_b values of NPPs were in the range between 6.76 and 13.2,

suggesting that NPPs had slightly weak or moderate bonding capacity within the scope of the material library.

Tabletability is the ability of a material to be densified into a compact with specific strength (Sun and Grant, 2001). Values of the tabletability descriptor d from the Power equation varied from 9.26×10^{-4} (Mume Fructus, No.Z6) to 1.19 (MCC type 102, No.E2), and values of the pressure sensitivity descriptor g varied from 0.249 to 1.68. According to the classification criteria with respect to the parameter d (Dai et al., 2019a), the tabletability of different powders can be divided into three categories, as shown in Table 2. 20 materials were distributed in Categories 1 and 2A, suggesting that they had good tabletability. Seven cellulose materials (i.e. 5 types of MCC, HPMC, and L-HPC) could reach tablet tensile strengths higher than 2.0 MPa at compression pressures lower than 50 MPa. The Lac 21 AN (No. E6) belonged to Category 2A material, demonstrating it offered the best tabletability among all grades of lactose applied. The Lac F100 and Lac G200 had Category 2B tabletability. Two types of lactose (i.e. Lac P200M and Lactose Tablettose 80 that was abbreviated as Lac T80), NaHCO_3 and DCP were classified as Category 2C materials, meaning that they could not meet the requirements for tablet tensile strength (i.e. $\text{TS} \geq 2.0$ MPa) even at high compression pressures. Particularly, it was observed that the pressure sensitivity descriptor g had a certain impact on the classification results. When the g value exceeded 1.5, the material could own the Category 2 properties even if the d value was $<2 \times 10^{-3}$. For example, despite having a g value of 1.68 and a d value of 9.26×10^{-4} , Mume Fructus (No. Z6) was classified as a Category 2A material, because it could be applied to produce tablets with $\text{TS} > 2.0$ MPa at the compression pressure of 50–100 MPa. This result suggested that the criteria for tabletability classification could be further improved by considering the g values of the Power equation.

3.3. Compaction behavior of granules

According to Section 2.3, two fractions of granules were collected for each material. The granules in the size fractions of 125–250 μm and 630–850 μm were called small granules and large granules in the following analysis, respectively. The compression equations in Table 1 were used to derive the CBCS parameters of small granules and large granules, respectively. By comparing the CBCS parameters of the granules with those of ungranulated powders, it was possible to examine how the compaction behavior of the materials changed after RCDG. A further comparison of the CBCS parameters between small granules and large granules could help investigate how granules particle size affected the change of compaction behavior.

3.3.1. From powders to small granules

In order to visualize the compaction behavior changes overall, a combinational dataset [62 \times 9] consisted of 9 CBCS parameters for 31 powders and 31 small granules was created. Then, the PCA was performed on this grouped dataset after the data preprocessing. It was found that 43.6% and 34.2% of the variation were explained by the first and second principal components, respectively. The third principal component explained only 7.24% of the variation, and the corresponding eigenvalue was <1 . As a result, the first two PCs were chosen for building the PCA model.

Fig. 4(A) shows the score plot of ungranulated powders and small

Table 2
The tabletability classification results of 31 materials.

Category	Category criteria	Subcategory	Number of materials
1	$d \geq 0.5$		6
2	$2 \times 10^{-3} \leq d < 0.5$	2A	14
		2B	6
3	$d < 2 \times 10^{-3}$	2C	4
			1

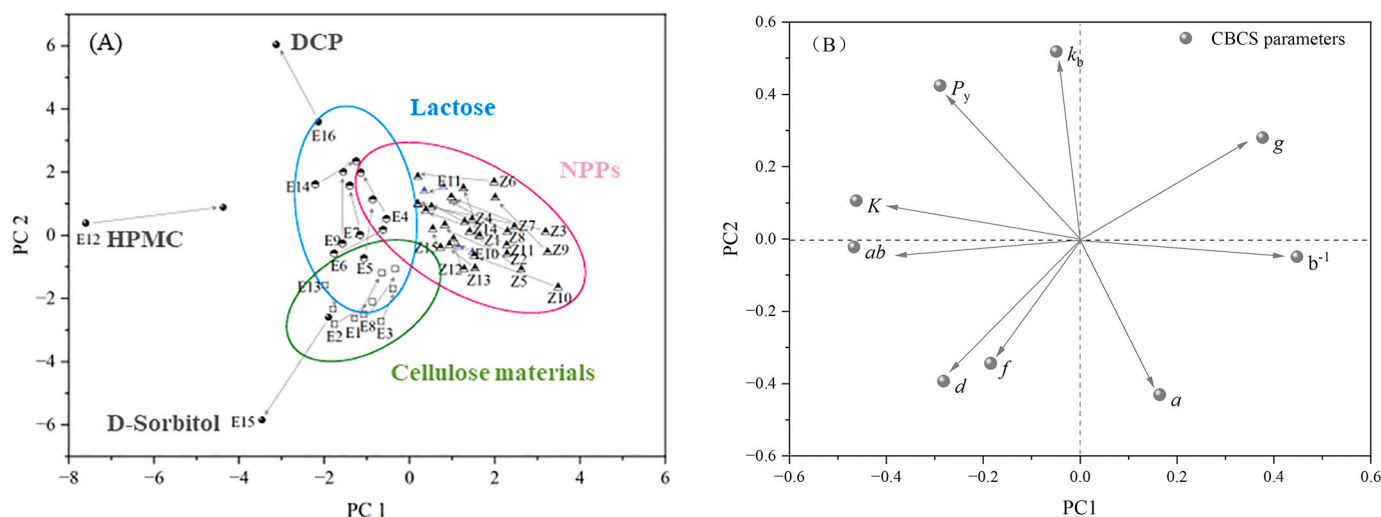


Fig. 4. The PCA analysis of the CBCS parameters for raw powders and small granules. (A) The score plot; (B) the loading plot.

granules, where the arrows represent the compaction behavior change from powders to small granules. As seen from Fig. 4(A), 31 materials are classified into three clusters together with three “outlier” samples. The three clusters were aggregation of cellulose materials, lactose materials and NPPs materials, respectively. The three “outlier” samples were HPMC (No. E12), D-Sorbitol (No. E15) and DCP (No. E16), which had significant changes of compaction behavior in terms of the arrow length. The D-Sorbitol and the L-HPC showed an increase of tableability since the *d* values of the two materials were increased. The particle sizes of small granules of D-Sorbitol were smaller than the particle size of its ungranulated powders (i.e. $D_{50} = 376.7 \mu\text{m}$). The decreased particle size increased the bonding area of D-Sorbitol granules, resulting in enhanced tablet tensile strength (Castaneda Hernandez et al., 2021). The HPMC possessed the highest *K* and *ab* values, and the arrow pointing at the HPMC granules indicated that the compressibility and rearrangement ability of HPMC were deteriorated after dry granulation. The group of cellulose materials contained 5 materials with good tableability, plastic deformation ability, and strong interparticle bonding ability. After RCDG, the group of the cellulose materials moved toward the upper right direction in the score plot, losing tableability and interparticle bonding capacity. However, the locations of powders and granules for cellulose group of materials were closer to the *d* variable than other materials, demonstrating that the LoT did not deteriorate the overall

tableability of them. The brittle materials like DCP and lactose had relatively high P_y and k_b values. As revealed by the direction of the arrow, both the compressibility and the bonding capacity of brittle materials were furtherly decreased after dry granulation. Besides, RCDG significantly weakened the plastic deformation and interparticle bonding properties of NaHCO_3 (No. E14). In the cluster of NPPs were all kinds of NPPs and 2 batches of excipients (i.e. CCNa and corn starch). The NPPs materials were in the positive direction of the PC1-axis, showing that they had good compressibility and plastic deformation ability, but were less likely to be rearranged during the compression process.

3.3.2. From small granules to large granules

Like Section 3.3.1, a combinational dataset [62 × 9] consisted of 9 CBCS parameters for 31 small granules and 31 large granules was created. Then, the PCA was carried out on this dataset after data pre-processing. The PC1, PC2 and PC3 explained 39.9%, 35.5% and 12.5% of the total variance in the data, respectively, and the first two PCs were selected to create a PCA model with 75.4% of the total explained variance.

Fig. 5(A) shows the score plot of the PCA model. Similar to Fig. 5(A), the materials could also be divided into three clusters and three pseudo-outliers. Among the three “outlier” samples, the arrow lengths of D-

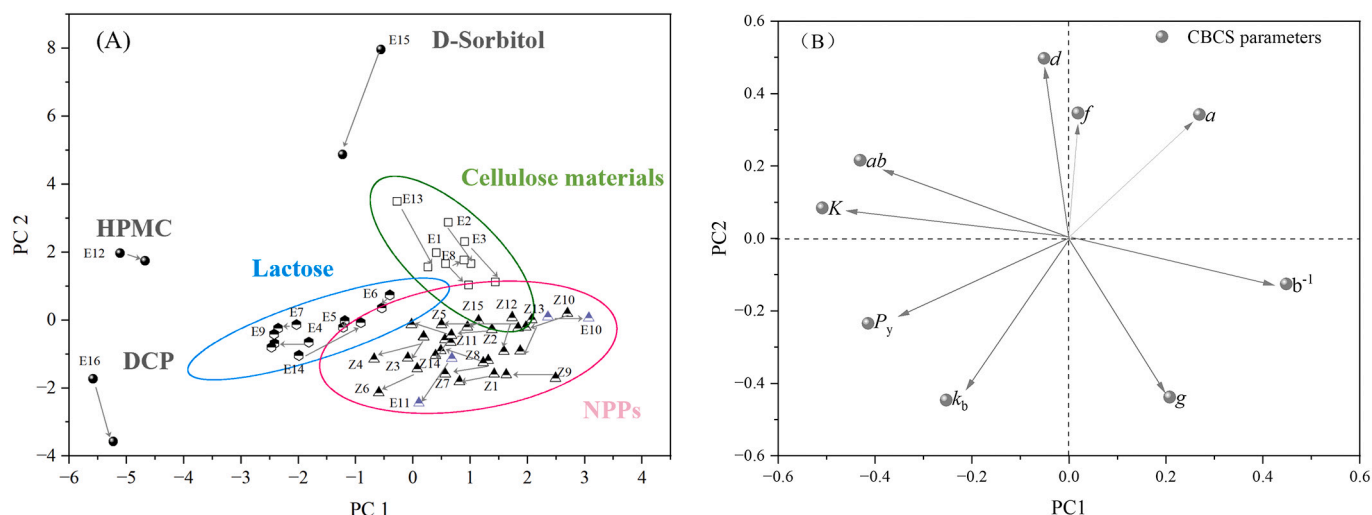


Fig. 5. The PCA analysis of the CBCS parameters for small granules and large granules. (A) The score plot; (B) the loading plot.

sorbitol and DCP were very long, revealing a considerable change in their compression behavior. For instance, the bonding force between the large D-sorbitol granules was weakened in comparison to that between the small D-sorbitol granules. And the tableability of DCP in the form of large granules was better than that in the form of small granules. The compaction behavior of HPMC did not change significantly with increasing granule sizes. For cellulose materials in the green circle, it seemed that the materials were moving toward the lower right side of the latent variable space, and this suggested that the tableability of cellulose materials decreased and the pressure sensitivity of them increased with increased granule sizes. The lactose materials, however, are not significantly affected by the increase in granule sizes, as evidenced by their short arrow lengths. Particularly, NaHCO_3 was in the blue circle, and the P_y and K_b values of large NaHCO_3 granules were smaller than those of small NaHCO_3 granules, implying that the plasticity and bonding capacity were improved after further granule size growth. On the contrary, for NPPs materials in the red circle, the main effects of granule particle size on the materials' compaction behavior were the further reduction in the plasty and bonding capacity.

3.4. Classification of tableability change

In Section 3.3, it was seen that different materials could be clustered according to their compression behaviors. In this Section, the change of tableability will be thoroughly discussed in terms of classification. Classifying involved using features to sort the material library into different groups or categories, which facilitated us to better understand the relationships between materials.

3.4.1. Qualitative analysis

The tableability of both powders and granules could be categorized according to the CBCS classification criteria for the parameter d . In cases powders are granulated into small granules, the tableability categories for 12 materials are altered as shown in Fig. 6(A). The tableability categories for ungranulated powders and small granules can be seen in Table S4 in Supplementary Materials. Among them, 3 materials, such as MCC PH102 SCG (No. E1), MCC PH102 (No. E3), and MCC PH302 (No. E8), changed the tableability categories from Category 1 to Category 2A. By contrast, the *Scutellariae Radix* (No. Z15) displayed an increase of tableability after RCDG, with its tableability category being raised from Category 2B to Category 2A. Besides, there were 4 materials whose tableability categories were changed from Category 2A to Category 2B, and there were 4 materials whose tableability categories were turned from Category 2B to Category 2C.

In cases powders were granulated into large granules, the tableability categories for 21 materials were altered after RCDG. The tableability categories for large granules can be seen in Table S5 in

Supplementary Materials. As shown in Fig. 6(B), it is clear that the tableability categories of more materials (i.e. No. E6, E10, Z1-Z7, Z9, Z12, and Z13) are changed from Category 2A to Category 2B. The tableability categories for *Chuanxiong Rhizoma* (No. Z5) and *Mume Fructus* (No. Z6) were decreased by two levels, i.e., from Category 2A to Category 2C, indicating that the two materials suffered from a high degree of LoT after RCDG. 13 kinds of large granules could not achieve the target of tablet tensile strength (i.e. 2.0 MPa) over the pressure range investigated. The results confirmed that RCDG usually led to tablets with reduced tensile strength, and the risk of tableability reduction was increased with the granule size enlargement.

3.4.2. Quantitative analysis

In order to quantify the degree of change of tableability, the CoT_r index was calculated using the methods in Section 2.7. Based on CoT_r values, the behavior of tableability change for all materials can be classified into three types, and the proposed tableability change classification system (TCCS) for RCDG is shown in Fig. 7. The first type (i.e. Type I) was featured by $CoT_r \leq -5\%$, and materials falling into Type I had the performance of LoT. The change of tableability for Type I materials could be further divided into two sub-types, i.e. Type Ia and Type Ib. The CoT_r values of Type Ia materials were less than or equal to -15% . The materials with CoT_r values ranging from -15% to -5% (including -5%) belonged to Type Ib. In other words, Type Ia materials had larger tableability reduction than Type Ib materials. The Type II materials was featured by $-5\% < CoT_r \leq 5\%$. The tableability of Type II materials had little change after RCDG, and the effect of the change of tableability on the tablet tensile strength could be ignored. The Type III materials were characterized by $CoT_r > 5\%$, which meant they had increased tableability after RCDG.

Fig. 7(A) depicts the CoT_r values of 31 materials under conditions of being granulated as small granules, which vary from -41.34% to 11.96% . There were 20 Type I materials. Among them, 8 materials were classified into Type Ia, including six batches of excipients and two batches of NPPs. The Type Ia excipients involved 5 kinds of cellulose excipients, such as MCC PH102SG (E1, $CoT_r = -41.34\%$), MCC type 102 (E2, $CoT_r = -31.40\%$), MCC PH302 (E8, $CoT_r = -32.78\%$), MCC PH102 (E3, $CoT_r = -16.06\%$), and HPMC (E12, $CoT_r = -16.04\%$). The granule hardening caused by the roll compaction increased the resistance to plastic deformation, thus leading to a large LoT of the MCC materials (Skelbaek-Pedersen et al., 2021). The D-sorbitol (E15, $CoT_r = -16.22\%$) also belonged to Type Ia. Two batches of NPPs, i.e. *Polygoni Multiflori Radix Praeparata* (No. Z9) and *Cinnamomum Cassia* (No. Z13), pertained to Type Ia and their CoT_r values were -29.31% and -15.77% , respectively. A total of 12 materials including 5 excipients and 7 NPPs were classified into Type Ib materials. It could be seen that most of lactose (i.e. 3 kinds out of 5), NaHCO_3 and CCNa belonged to Type Ib

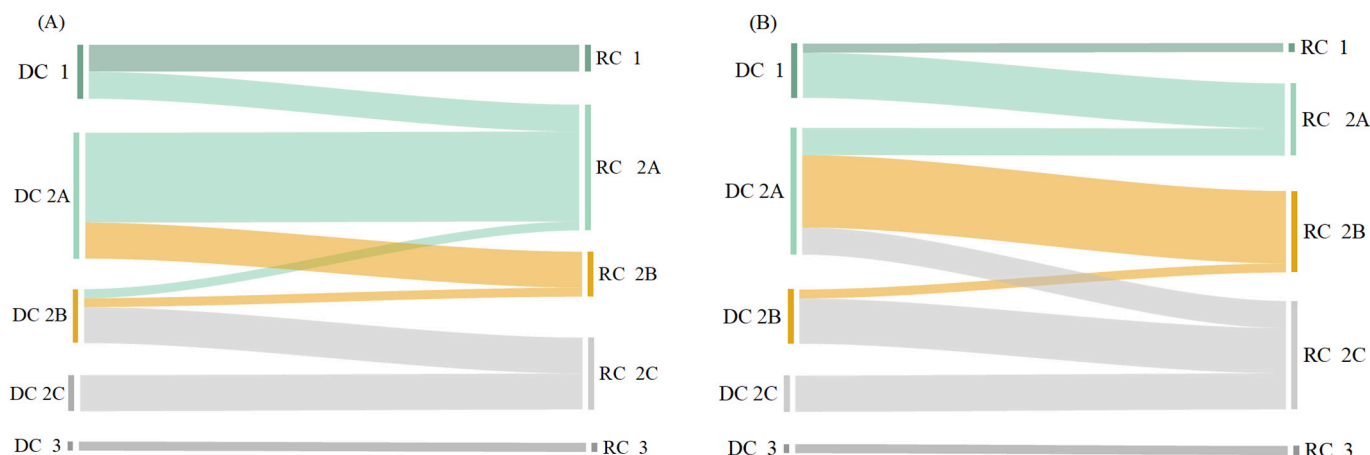


Fig. 6. Change of tableability categories (A) from powders to small granules and (B) from powders to large granules.

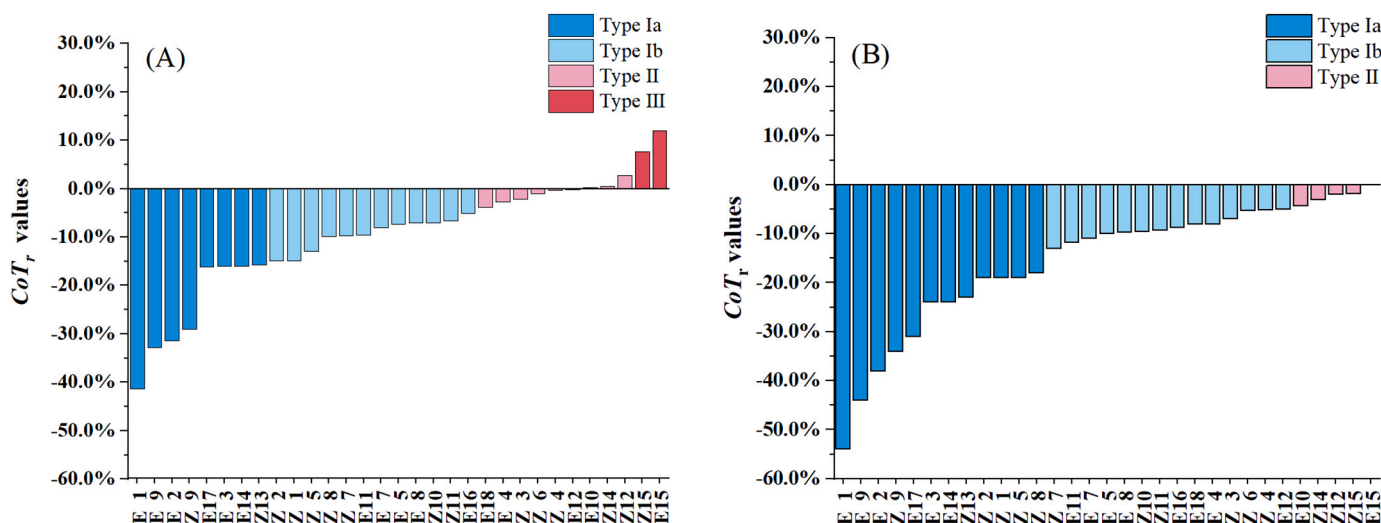


Fig. 7. The tabletability change classification system. (A) The CoT_r values and tabletability change classification results for materials granulated as small granules; (B) the CoT_r values and tabletability change classification results for materials granulated as large granules.

powders. The three batches of lactose had similar CoT_r values, which were -8.09% (Lac 21AN), -7.33% (Lac F100) and -7.04% (Lac G200).

9 materials including 4 excipients and 5 NPPs were within the Type II group. The CoT_r values of Type II materials ranged from -3.85% (DCP) to 2.78% (Sophorae Flavescentis Radix, No. Z12). The excipients belonging to Type II were the remaining 2 batches of lactose (i.e. Lac T80 and Lac P200M), corn starch and DCP. Generally, the tensile strength variation of a Type II material was not prominent before and after the RCDG process. Only 2 materials that were L-HPC ($CoT_r = 11.96\%$) and Scutellariae Radix (No. Z15, $CoT_r = 7.63\%$) belonged to Type III. As revealed by the CBCS parameters for the L-HPC, both the compressibility and compactibility of the L-HPC granules were improved by RCDG.

Fig. 7(B) depicts the CoT_r values of 31 materials under conditions of being granulated as large granules, which vary from -53.94% to -0.06% . 26 materials were classified as Type I, and none of them displayed improved tabletability. 12 materials including seven excipients and five NPPs were furtherly classified into Type Ia. Within this group, five granules such as four batches of MCC (No. E1, E2, E3, and E9) and Polygoni Multiflori Radix Praeparata (No. Z9) had $>30\%$ reduction in relative tabletability. Only 5 batches of materials fell into type II. Conventionally, the size enlargement and thereby reduced bonding area between granules were considered as a factor influencing the tabletability of dry granules. In our case, the difference between CoT_r value for a material granulated as large granules and CoT_r value for the same material granulated as small granules was calculated, and such difference values for 11 materials including 8 excipients and 3 NPPs were $<3\%$. For instance, the CoT_r values of Lac T80 granulated as small granules and large granules were -7.33% and -8.71% , respectively. This phenomenon indicated that the tabletability of these 11 materials was less affected by a further granule size enlargement during RCDG.

3.5. The risk decision tree for material's tabletability in RCDG

Practically, more than one material will be involved in a tablet formulation, and the effects of additional factors such as the proportion or the function of a component on the final tablet tensile strength should be considered. Based on the comprehensive analysis of the tabletability category and the tabletability change type for all materials in the material library, a decision tree for risk evaluation of a material's tabletability in RCDG is brought forward as shown in Fig. 8. The decision tree is established with small granules data and is validated with large granules data, which are shown in Table S4 and Table S5 in

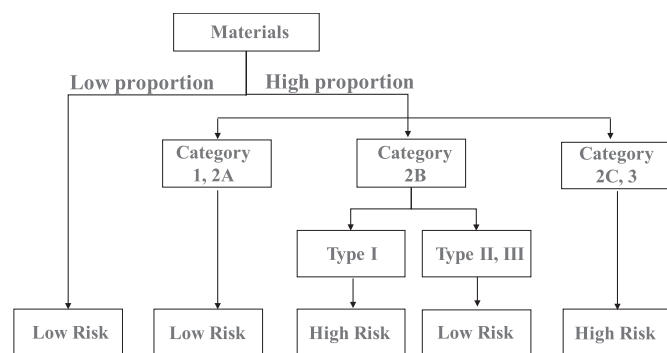


Fig. 8. The risk decision tree for evaluation of a material's tabletability in RCDG.

Supplementary Materials.

If the proportion of a powdered material in tablet formulation was low, it may not pose any risk to tablet tensile strength. For instance, the disintegrants such as CCNa and L-HPC in the established material library were typically used in small amounts ranging from 2% to 5% in formulations (Gamble et al., 2010; Jeon and Betz, 2011). Therefore, the contribution of disintegrants to the tabletability reduction of the whole mixture would be weak. Moreover, a study had reported that the intra-granular addition of super disintegrants (i.e. croscarmellose sodium and sodium starch glycolate) could compensate the loss of compactibility of anhydrous lactose-based granules produced via RCDG (Jaspers et al., 2022).

If the proportion of a powdered material such as filler or diluent in tablet formulation was high, the tabletability of powdered materials could help make further decisions when evaluating the potential risk of the occurrence of decreased tabletability. For materials belonging to Category 1 or Category 2A, even if they had a Type Ia or Type Ib change of tabletability, the re-compactibility was still favorable since the produced granules all had good tabletability. In other words, the risk for the occurrence of unwanted tablet tensile strength was low when high proportions of Category 1 or 2A materials were involved in dry granulation formulations. For materials belonging to Category 2C or Category 3, the primary deficiency in tabletability would be inevitably transferred into the intermediate granules, and the high proportion of these materials may result in unacceptable tablet tensile strength.

For materials belonging to Category 2B, it depended on the change of

tableability. If the Type I change of tableability happened on a material, the risk of tablet failure was high. For example, the tableability of *Notopterygii Rhizoma Et Radix* (Z11, $CoT_r = -6.62\%$) was classified as Category 2B. After RCDG, the tableability of corresponding granules was classified as Category 2C, which suggested that the tablet tensile strength could not meet the requirements. Nevertheless, If the Type II or Type III change of tableability happened on a material, there would be no risk to be considered, because the granules still maintained the classification of tableability of powders after dry granulation.

The tablet categories and tableability change types for large granules were used to validate the accuracy of the decision tree. For example, the tableability category of *Visci Herba* (No. Z2) powder was 2A, and the tableability change type was Ia. If the *Visci Herba* was used in high proportion, the related risk was decided to be low. In reality, the tableability category of *Visci Herba* granules was 2B, which meant acceptable tablet tensile strength would be obtained at high compression pressure. The judgments were performed for all materials, and the decision accuracy reached 90.3%. For *Menthae Haplocalycis Herba* (No. Z14), the risk decision result was low, because its tableability category and the tableability change type were 2B and II, respectively. Nevertheless, the tableability category of *Menthae Haplocalycis Herba* granules was 2C, meaning that acceptable tablet tensile strength (≥ 2.0 MPa) would not be obtained even at high compression pressures. After further looking at the tableability curve of *Menthae Haplocalycis Herba* granules, it was found that the tablet tensile strength could reach 1.88 MPa at the compression pressure of 140 MPa. According to the manufacturing classification system (Leane et al., 2015), the tablet with tensile strength ≥ 1.7 MPa would be robust to further processing. Therefore, the risk decision result for *Menthae Haplocalycis Herba* material was reasonable. Under the pressure of 140 MPa, two category 2A materials that were wrongly classified as low-risk could obtain tablets with tensile strength >1.7 MPa. Therefore, it could be concluded that the decision tree is reliable in its judgment results. The decision tree for risk analysis of a material's tableability could be used as a reference for formulation design in the dry granulation and tableting processes. Anyway, for high-risk materials, their proportions in drug product should be paid attention, and a balanced performance was required in the tablet formulation design.

3.6. Comparison of the material property design space for DC and RCDG toward tablet manufacturing

With the help of predictive modeling, it was possible to identify the different requirements for material properties in different tablet manufacturing routes, which were DC and RCDG in this paper. Since the granules with size fractions 630–850 μm were not suitable for tablet production, the small granules were used to establish the predictive model. In addition to 18 physical properties and 9 CBCS parameters that described the material properties, CoT_r and RP were also employed as material property descriptors, and the latter two indexes possessed the advantage that they reflected the tableability change of a material under a given set of process conditions of RCDG. For simulating the tableting process, 5 compression forces (i.e. 3, 5, 7, 9 and 11 kN) within the compression pressure range were defined, and the corresponding table tensile strength could be calculated from the fitted Power equations for either powders or granules. For 31 materials with each material being compressed at 5 different pressures, a total of 155 observations (31 \times 5) could be obtained. For each observation, the 29 material properties and the compression pressure are combined as input variables, and the tensile strength of both DC tablet (TS_1) and RCDG tablet (TS_2) are used as output variables, as shown in Table 3.

The PLS2 regression was used to relate the input and output variables. Three indicators, i.e. the fraction of the variation of the X variables explained by the model (R^2X), the fraction of the variation of the Y variables explained by the model (R^2Y) and the fraction of the variation of the Y variables predicted by the model (Q^2Y), were used to evaluate

Table 3 The input and output variables for the partial least squares (PLS2) model.

Type of variable	Variables	
Input variable	Material properties	$D_b, D_c, \rho_b, I_e, IC, Icd, IH, AoR, t'', \%HR, \%H, \%pf, I\theta, D_{10}, D_{50}, D_{90}, Span, SF_p$
	CBCS descriptors	$P_y, a, b^{-1}, ab, K, k_b, f, d, g$
	Tableability change indexes	CoT_r, RP
	Compaction pressure	P
Output variable	Tablet property	TS_1, TS_2

the quality of the model and served as the basis for model optimization. The model metrics for the built PLS model showed that when the first four latent variables were selected, the R^2Y_{cum} and Q^2Y_{cum} were 91.9% and 89.5%, respectively, but the R^2X_{cum} was only 60.9%. The fifth latent variable did not significantly improve the R^2Y_{cum} and Q^2Y_{cum} values of the model but could raise the R^2X_{cum} to 73.5%. Therefore, five latent variables were selected to build the model, and the R^2Y_{cum} and Q^2Y_{cum} of the final model were 92.3% and 89.7%, respectively. This demonstrated that the built PLS model had good performance in predicting the tablet quality. Fig. 9 is the loading plot under the first two latent variables. TS_1 and TS_2 were situated near each other, and the correlation coefficient between them was 0.919. This suggested that the compaction of the roller compacted granules to form tablets is closely related to the compaction of the primary particles (Farber et al., 2008; Shi and Hilden, 2017). It can be seen from Fig. 9 that, $Icd, d,$ and P are strongly positively correlated with TS_1 and TS_2 . While, the compaction descriptors (K_b, P_y) and the density related parameters (D_b and D_c) are negatively correlated with TS_1 and TS_2 . In addition, the CoT_r index had a strong negative correlation with TS_1 and TS_2 , demonstrating that the CoT_r index succeeded in predicting the tablet tensile strength. However, the RP was located near the center of the loading plot, indicating that it contributed little to the prediction of tablet quality.

By setting the targets for TS_1 and TS_2 of tablets, the area that met tablet requirements in the latent variable space could be visualized in the score plot. As shown in Fig. 10, the green and blue lines correspond to $TS_1 = 2.0$ MPa and $TS_2 = 2.0$ MPa, respectively. The area within the 95% confidence ellipse and above the green and blue lines were regions for DC tablets and RCDG tablets that met the tensile strength requirements, respectively. The semi-ellipse region for DC was larger than that for RCDG, which was attributed to the phenomenon of LoT during RCDG. As discussed in Section 3.1, powdered materials with D_b higher

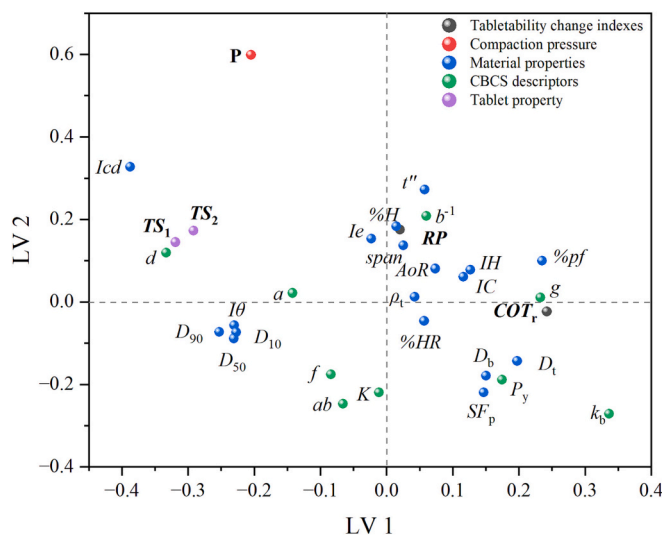


Fig. 9. The loading plot for the PLS model based on the first two latent variables.

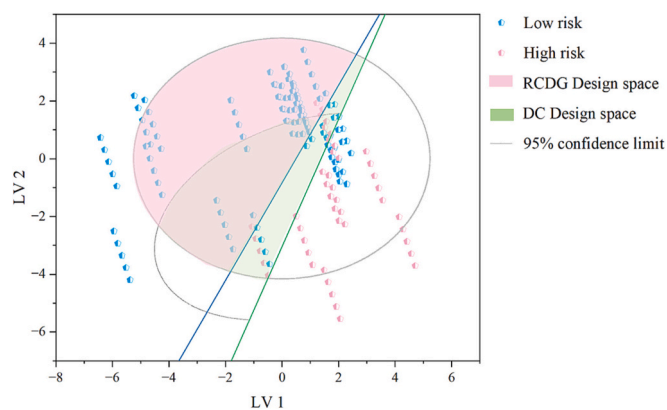


Fig. 10. The design space developed based on the PLS model. (The green line represents $TS_1 = 2.0$ MPa, and the blue line represents $TS_2 = 2.0$ MPa. The green area represents the DC design space, and the red area represents the RCDG design space.) (For interpretation of the references to colour in this figure legend, the reader is referred to the web version of this article.)

than $0.5 \text{ g}\cdot\text{mL}^{-1}$ are suitable for DC. This constraint was added to the score plot by drawing the 95% confidence ellipse on the powders with D_b higher than $0.5 \text{ g}\cdot\text{mL}^{-1}$, and the intersectional green area represented the DC design space. This enabled the subdivision of the developability space into areas represented by DC and RCDG. The RCDG design space covered more materials than the DC design space and the RCDG processing route could be used to manufacture tablets with lower D_b materials. Assuming that all materials were used in high proportions, and the related risk could be estimated by the decision tree in Fig. 8. The materials with a high risk of LoT are represented by red dots in Fig. 10. It could be seen that most of the red dots were distributed on the right side of the target line of RCDG. This demonstrated that the proposed decision tree provided an easy and reliable pathway to a decision, when selecting materials for tablet formulation design. Considering the LoT, selecting the starting materials with good bonding capacity or tabletability was beneficial to achieve the target of tablet tensile strength.

4. Conclusion

In this paper, a material library containing 31 materials was built and comprehensively characterized. The univariate distribution analysis and the principal component analysis revealed that the built material database was full of diversity, and the natural product powders complemented the material property space of the pharmaceutical excipients. By applying a moderate roll compression force, the primary powders were designed to be granulated as small granules and large granules, respectively. Both the powders and granules were characterized by 9 CBCS parameters. The changes in the compression behaviors from powders to granules were investigated by the principal component analysis. Generally, the RCDG process deteriorated the tabletability of cellulose materials, the bonding capability of lactose materials and the plastic deformability of natural product materials. A further granules size enlargement did not impact the compaction behavior of lactose materials, but could increase the compressibility and rearrangement ability of natural product materials and decrease the plasticity and bonding capacity of cellulose materials.

The change of tabletability was studied by both the qualitative and quantitative classification methods. With the help of the CoT_r index, the TCCS was successfully built. The tabletability change of 31 materials could be classified into three groups, i.e. the loss of tabletability, the unchanged of tabletability and the increase of tabletability. Under the conditions of being granulated as small granules, 20 out of 31 materials exhibited the loss of tabletability. While, under the conditions of being granulated as large granules, 26 out of 31 materials showed tabletability reduction. These results demonstrated the prevalent loss of tabletability

phenomenon. However, the loss of tabletability of a material may not pose a threat to the final tablet tensile strength. In order to aid decision making in tablet formulation design, a risk decision tree was innovatively developed by the joint application of the CBCS tabletability categories and the TCCS tabletability change types. Attentions should be paid to the Category 2C and Category 3 materials, as well as the Category 2B materials with Type I change of tabletability, when the proportions of these materials were relatively high in tablet formulation. Furthermore, by using data fusion and the partial least squares modeling technique, the material property design space for DC and RCDG could be identified in the latent variable space, which agreed with the risk analysis results.

In this paper, only the single materials and the fixed process conditions were used to explore the tabletability change under RCDG. In practice, both the formulation compositions and the RCDG process parameters could impact the material's change of tabletability. The following studies will investigate the impact of interactions between the material properties space and the process parameters space on the change of tabletability, and construct a more versatile design model for accelerating the tablet formulation and process design via the manufacturing route of dry granulation.

Funding sources

This research was funded by the National Natural Science Foundation of China (No. 82074033).

CRediT authorship contribution statement

Junhui Su: Investigation, Formal analysis, Writing – original draft. **Kunfeng Zhang:** Investigation, Validation. **Feiyu Qi:** Visualization. **Junjie Cao:** Data curation. **Yuhua Miao:** Writing – review & editing. **Zhiqiang Zhang:** Resources. **Yanjiang Qiao:** Supervision. **Bing Xu:** Conceptualization, Writing – review & editing, Funding acquisition.

Declaration of Competing Interest

The authors declare the following financial interests/personal relationships which may be considered as potential competing interests:

Bing Xu reports equipment, drugs, or supplies was provided by We acknowledge the natural product samples provided by Beijing Tcmages Pharmaceutical Co., Ltd.

Data availability

I have shared the data at the attach files.

Acknowledgements

We acknowledge the natural product samples provided by Beijing Tcmages Pharmaceutical Co., Ltd.

Appendix A. Supplementary data

Supplementary data to this article can be found online at <https://doi.org/10.1016/j.ijpx.2023.100204>.

References

- Atanasov, A.G., Zotchev, S.B., Dirsch, V.M., et al., 2021. Natural products in drug discovery: advances and opportunities. *Nat. Rev. Drug Discov.* 20, 200–216. <https://doi.org/10.1038/s41573-020-00114-z>.
- Basu, P.K., Khan, M.A., Hoag, S., et al., 2011. NIPTE-FDA Excipients Knowledge Base.
- Castaneda Hernandez, O., Caraballo Rodriguez, I., Bernad Bernad, M.J., et al., 2021. Comparison of the performance of two grades of metformin hydrochloride elaboration by means of the SeDeM system, compressibility, compactability, and process capability indices. *Drug Dev. Ind. Pharm.* 47, 484–497. <https://doi.org/10.1080/03639045.2021.1892741>.

- Dai, S., Xu, B., Zhang, Z., et al., 2019a. A compression behavior classification system of pharmaceutical powders for accelerating direct compression tablet formulation design. *Int. J. Pharm.* 572, 118742 <https://doi.org/10.1016/j.ijpharm.2019.118742>.
- Dai, S.Y., Xu, B., Shi, G.L., et al., 2019b. SeDeM expert system for directly compressed tablet formulation: a review and new perspectives. *Powder Technol.* 342, 517–527. <https://doi.org/10.1016/j.powtec.2018.10.027>.
- Dhondt, J., Bertels, J., Kumar, A., et al., 2022a. A multivariate formulation and process development platform for direct compression. *Int. J. Pharm.* 623, 121962 <https://doi.org/10.1016/j.ijpharm.2022.121962>.
- Dhondt, J., Eeckhout, Y., Bertels, J., et al., 2022b. A multivariate methodology for material sparing characterization and blend design in drug product development. *Int. J. Pharm.* 621, 121801 <https://doi.org/10.1016/j.ijpharm.2022.121801>.
- Farber, L., Hapgood, K.P., Michaels, J.N., et al., 2008. Unified compaction curve model for tensile strength of tablets made by roller compaction and direct compression. *Int. J. Pharm.* 346, 17–24. <https://doi.org/10.1016/j.ijpharm.2007.06.022>.
- Fell, J.T., Newton, J.M., 1970. Determination of tablet strength by the diametral-compression test. *J. Pharm. Sci.* 59, 688–691. <https://doi.org/10.1002/jps.2600590523>.
- Gamble, J.F., Tobyn, M., Dennis, A.B., et al., 2010. Roller compaction: application of an in-gap ribbon porosity calculation for the optimization of downstream granule flow and compactability characteristics. *Pharm. Dev. Technol.* 15, 223–229. <https://doi.org/10.3109/10837450903095342>.
- Grote, S., Kleinebudde, P., 2018. Roll Compaction/Dry Granulation of Dibasic Calcium Phosphate Anhydrous—does the Morphology of the Raw Material Influence the Tableability of Dry Granules? *J. Pharm. Sci.* 107, 1104–1111. <https://doi.org/10.1016/j.xphs.2017.12.003>.
- Grote, S., Kleinebudde, P., 2019. A comparative study of the influence of alpha-lactose monohydrate particle morphology on granule and tablet properties after roll compaction/dry granulation. *Pharm. Dev. Technol.* 24, 314–322. <https://doi.org/10.1080/10837450.2018.1476977>.
- Hancock, B.C., 2019. The Wall Friction Properties of Pharmaceutical Powders, Blends, and Granulations. *J. Pharm. Sci.* 108, 457–463. <https://doi.org/10.1016/j.xphs.2018.10.019>.
- Hayashi, Y., Nakano, Y., Marumo, Y., et al., 2021. Application of machine learning to a material library for modeling of relationships between material properties and tablet properties. *Int. J. Pharm.* 609, 121158 <https://doi.org/10.1016/j.ijpharm.2021.121158>.
- Heiman, J., Tajarobi, F., Gururajan, B., et al., 2015. Roller compaction of hydrophilic extended release tablets—combined effects of processing variables and drug/matrix former particle size. *AAPS PharmSciTech* 16, 267–277. <https://doi.org/10.1208/s12249-014-0219-3>.
- Hein, S., Picker-Freyer, K.M., Langridge, J., 2008. Simulation of roller compaction with subsequent tableting and characterization of lactose and microcrystalline cellulose. *Pharm. Dev. Technol.* 13, 523–532. <https://doi.org/10.1080/10837450802288972>.
- Herting, M.G., Kleinebudde, P., 2007. Roll compaction/dry granulation: effect of raw material particle size on granule and tablet properties. *Int. J. Pharm.* 338, 110–118. <https://doi.org/10.1016/j.ijpharm.2007.01.035>.
- Herting, M.G., Kleinebudde, P., 2008. Studies on the reduction of tensile strength of tablets after roll compaction/dry granulation. *Eur. J. Pharm. Biopharm.* 70, 372–379. <https://doi.org/10.1016/j.ejpb.2008.04.003>.
- Janssen, P.H.M., Jaspers, M., Meier, R., et al., 2022. The effect of excipient particle size on the reduction of compactibility after roller compaction. *Int. J. Pharm.* X 4, 100117 <https://doi.org/10.1016/j.ijpx.2022.100117>.
- Jaspers, M., Roelofs, T.P., Janssen, P.H.M., et al., 2022. A novel approach to minimize loss of compactibility in a dry granulation process using superdisintegrants. *Powder Technol.* 408 <https://doi.org/10.1016/j.powtec.2022.117773>.
- Jeon, I., Betz, G., 2011. Roll compaction as a dry granulation method for paracetamol. *J. Drug Deliv. Sci. Technol.* 21, 257–262. [https://doi.org/10.1016/S1773-2247\(11\)50035-8](https://doi.org/10.1016/S1773-2247(11)50035-8).
- Joiris, E., Di Martino, P., Berneron, C., et al., 1998. Compression behavior of orthorhombic paracetamol. *Pharm. Res.* 15, 1122–1130. <https://doi.org/10.1023/a:1011954800246>.
- Kleinebudde, P., 2004. Roll compaction/dry granulation: pharmaceutical applications. *Eur. J. Pharm. Biopharm.* 58, 317–326. <https://doi.org/10.1016/j.ejpb.2004.04.014>.
- Klevan, I., Nordstrom, J., Tho, I., et al., 2010. A statistical approach to evaluate the potential use of compression parameters for classification of pharmaceutical powder materials. *Eur. J. Pharm. Biopharm.* 75, 425–435. <https://doi.org/10.1016/j.ejpb.2010.04.006>.
- Kuntz, T., Schubert, M.A., Kleinebudde, P., 2011. Increased compactibility of acetames after roll compaction. *Eur. J. Pharm. Biopharm.* 77, 164–169. <https://doi.org/10.1016/j.ejpb.2010.09.013>.
- Leane, M., Pitt, K., Reynolds, G., et al., 2015. A proposal for a drug product Manufacturing Classification System (MCS) for oral solid dosage forms. *Pharm. Dev. Technol.* 20, 12–21. <https://doi.org/10.3109/10837450.2014.954728>.
- Li, Z., Wu, F., Zhao, L., et al., 2018. Evaluation of fundamental and functional properties of natural plant product powders for direct compaction based on multivariate statistical analysis. *Adv. Powder Technol.* 29, 2881–2894. <https://doi.org/10.1016/j.apt.2018.08.009>.
- Malkowska, S., Khan, K., 1983. Effect of re-compression on the properties of tablets prepared by dry granulation. *Drug Dev. Ind. Pharm.* 9, 331–347. <https://doi.org/10.3109/03639048309044678>.
- Nofrerias, I., Nardi, A., Sune-Pou, M., et al., 2018. Optimization of the Cohesion Index in the SeDeM Diagram Expert System and application of SeDeM Diagram: an improved methodology to determine the Cohesion Index. *PLoS One* 13, e0203846. <https://doi.org/10.1371/journal.pone.0203846>.
- Nordstrom, J., Alderborn, G., 2015. The granule porosity controls the loss of compactibility for both dry- and wet-processed cellulose granules but at different rate. *J. Pharm. Sci.* 104, 2029–2039. <https://doi.org/10.1002/jps.24439>.
- Nordstrom, J., Klevan, I., Alderborn, G., 2009. A particle rearrangement index based on the Kawakita powder compression equation. *J. Pharm. Sci.* 98, 1053–1063. <https://doi.org/10.1002/jps.21488>.
- Omar, C.S., Dhenge, R.M., Palzer, S., et al., 2016. Roller compaction: effect of relative humidity of lactose powder. *Eur. J. Pharm. Biopharm.* 106, 26–37. <https://doi.org/10.1016/j.ejpb.2016.02.016>.
- Palugan, L., Moutaharrik, S., Cirilli, M., et al., 2022. Evaluation of different types of mannitol for dry granulation by roller compaction. *J. Drug Deliv. Sci. Tech.* 75, 103619 <https://doi.org/10.1016/j.jddst.2022.103619>.
- Parikh, D.M., 2021. *Handbook of Pharmaceutical Granulation Technology*, 4 ed. CRC Press, Florida.
- Patel, S., Dahiya, S., Sun, C.C., et al., 2011. Understanding size enlargement and hardening of granules on tableability of unlubricated granules prepared by dry granulation. *J. Pharm. Sci.* 100, 758–766. <https://doi.org/10.1002/jps.22315>.
- Paul, S., Tajarobi, P., Boissier, C., et al., 2019. Tableting performance of various mannitol and lactose grades assessed by compaction simulation and chemometrical analysis. *Int. J. Pharm.* 566, 24–31. <https://doi.org/10.1016/j.ijpharm.2019.05.030>.
- Reynolds, G.K., Campbell, J.I., Roberts, R.J., 2017. A compressibility based model for predicting the tensile strength of directly compressed pharmaceutical powder mixtures. *Int. J. Pharm.* 531, 215–224. <https://doi.org/10.1016/j.ijpharm.2017.08.075>.
- Shi, Z., Hilden, J.L., 2017. Small-Scale Modeling of Pharmaceutical Powder Compression from tap Density Testers, to Roller Compactors, and to the Tablet Press using big Data. *J. Pharm. Innov.* 12, 41–48. <https://doi.org/10.1007/s12247-016-9267-4>.
- Skelbaek-Pedersen, A.L., Vilhelmsen, T.K., Rantanen, J., et al., 2021. The relevance of granule fragmentation on reduced tableability of granules from ductile or brittle materials produced by roll compaction/dry granulation. *Int. J. Pharm.* 592, 120035 <https://doi.org/10.1016/j.ijpharm.2020.120035>.
- Souhli, N., Dumarey, M., Wikstrom, H., et al., 2013. A quality by design approach to investigate the effect of mannitol and dicalcium phosphate qualities on roll compaction. *Int. J. Pharm.* 447, 47–61. <https://doi.org/10.1016/j.ijpharm.2013.02.036>.
- Sun, C.C., 2008. On the mechanism of reduced tableability of granules prepared by roller compaction. *Int. J. Pharm.* 347, 171–172 author reply 173–174. <https://doi.org/10.1016/j.ijpharm.2007.10.002>.
- Sun, C.C., 2011. Decoding Powder Tableability: Roles of Particle Adhesion and Plasticity. *J. Adhes. Sci. Technol.* 25, 483–499. <https://doi.org/10.1163/016942410x525678>.
- Sun, C., Grant, D.J., 2001. Influence of crystal structure on the tableting properties of sulfamerazine polymorphs. *Pharm. Res.* 18, 274–280. <https://doi.org/10.1023/a:1011038526805>.
- Sun, C.C., Himmelspach, M.W., 2006. Reduced tableability of roller compacted granules as a result of granule size enlargement. *J. Pharm. Sci.* 95, 200–206. <https://doi.org/10.1002/jps.20531>.
- Sun, C.C., Kleinebudde, P., 2016. Mini review: Mechanisms to the loss of tableability by dry granulation. *Eur. J. Pharm. Biopharm.* 106, 9–14. <https://doi.org/10.1016/j.ejpb.2016.04.003>.
- Suñé Negre, J.M., Roig, M., Fuster, R., et al., 2014. New classification of directly compressible (DC) excipients in function of the SeDeM Diagram Expert System. *Int. J. Pharm.* 470, 15–27. <https://doi.org/10.1016/j.ijpharm.2014.04.068>.
- Tofiq, M., Nordstrom, J., Persson, A.S., et al., 2022a. Deciphering the role of granule deformation and fragmentation for the tableting performance of some dry granulated powders. *Powder Technol.* 409, 117794 <https://doi.org/10.1016/j.powtec.2022.117794>.
- Tofiq, M., Nordstrom, J., Persson, A.S., et al., 2022b. Effect of excipient properties and blend ratio on the compression properties of dry granulated particles prepared from microcrystalline cellulose and lactose. *Powder Technol.* 399, 117207 <https://doi.org/10.1016/j.powtec.2022.117207>.
- Van Snick, B., Dhondt, J., Pandelaere, K., et al., 2018. A multivariate raw material property database to facilitate drug product development and enable in-silico design of pharmaceutical dry powder processes. *Int. J. Pharm.* 549, 415–435. <https://doi.org/10.1016/j.ijpharm.2018.08.014>.
- Vervae, C., Remon, J.P., 2005. Continuous granulation in the pharmaceutical industry. *Chem. Eng. Sci.* 60, 3949–3957. <https://doi.org/10.1016/j.ces.2005.02.028>.
- Wang, Y., O'Connor, T., Li, T., et al., 2019. Development and applications of a material library for pharmaceutical continuous manufacturing of solid dosage forms. *Int. J. Pharm.* 569, 118551 <https://doi.org/10.1016/j.ijpharm.2019.118551>.
- Wang, Y., Cao, J., Zhao, X., et al., 2022. Using a Material Library to Understand the Change of Tableability by High Shear Wet Granulation. *Pharmaceutics* 14 <https://doi.org/10.3390/pharmaceutics14122631>.
- Xiong, Z., Yang, B., Zhao, Y.X., et al., 2022. A new direct compression mechanism of structural transition in *Portia cocos* extract composite particles. *Int. J. Pharm.* 121913 <https://doi.org/10.1016/j.ijpharm.2022.121913>.
- Yu, J., Xu, B., Zhang, K., et al., 2019. Using a Material Library to Understand the Impacts of Raw Material Properties on Ribbon Quality in Roll Compaction. *Pharmaceutics* 11, 662. <https://doi.org/10.3390/pharmaceutics11120662>.
- Yu, Y., Zhao, L., Lin, X., et al., 2021. Research on the powder classification and the key parameters affecting tablet qualities for direct compaction based on powder functional properties. *Adv. Powder Technol.* 32, 565–581. <https://doi.org/10.1016/j.apt.2021.01.002>.
- Zhang, Y., Xu, B., Wang, X., et al., 2019. Optimal selection of Incoming Materials from the Inventory for Achieving the Target Drug Release Profile of High Drug load

Sustained-Release Matrix Tablet. AAPS PharmSciTech 20, 76. <https://doi.org/10.1208/s12249-018-1268-9>.
Zhang, Y., Li, J., Gao, Y., et al., 2022. Improvements on multiple direct compaction properties of three powders prepared from Puerariae Lobatae Radix using surface

and texture modification: Comparison of microcrystalline cellulose and two nano-silicas. Int. J. Pharm. 622, 121837 <https://doi.org/10.1016/j.ijpharm.2022.121837>.
Zhao, H., Shi, C., Liu, Z., et al., 2023. Evaluating the effect of Microcrystalline Cellulose Variations on Tablet Quality of Natural Plant Product using a Design of Experiment Approach. AAPS PharmSciTech 24. <https://doi.org/10.1208/s12249-023-02556-1>.